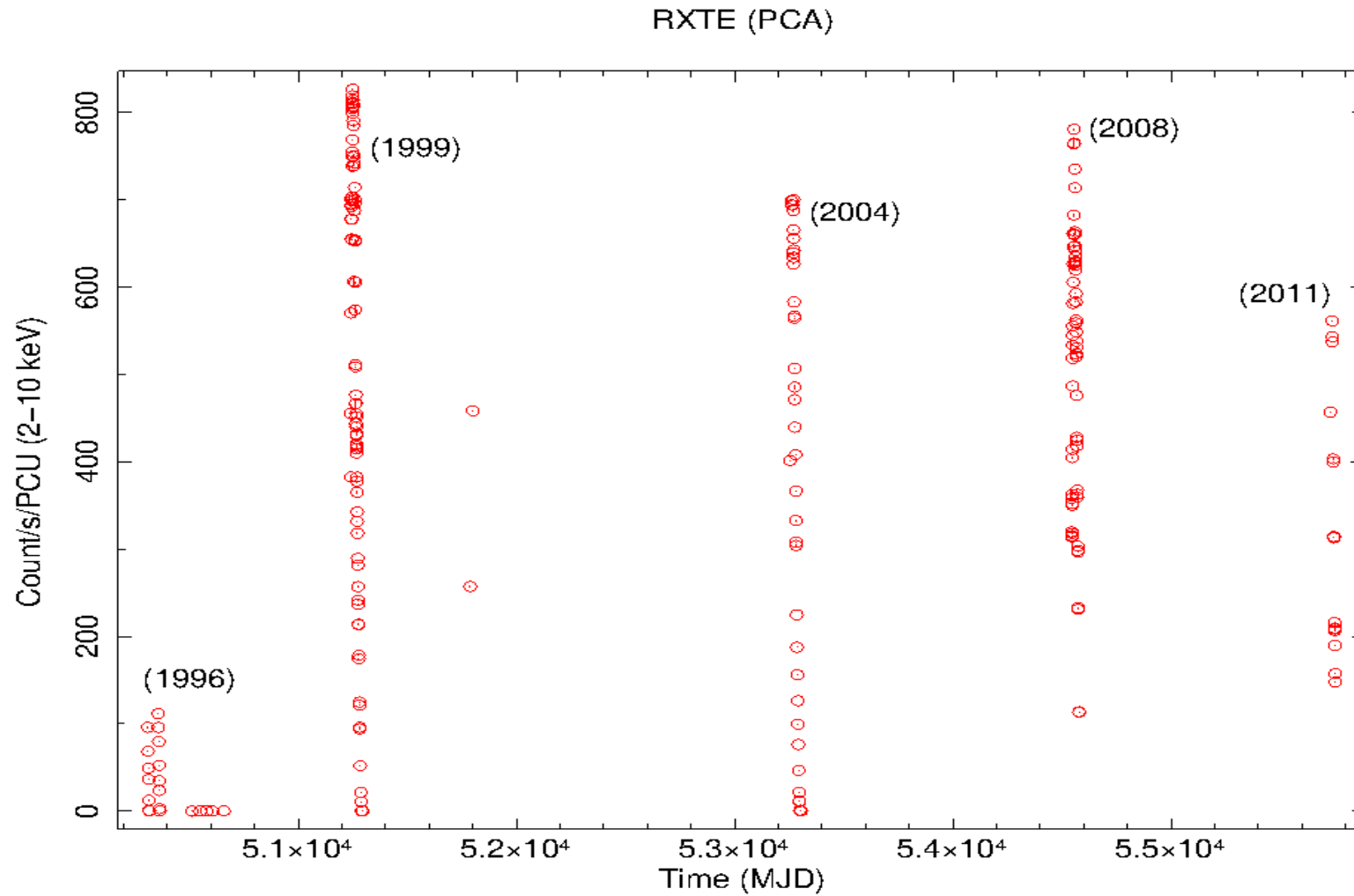


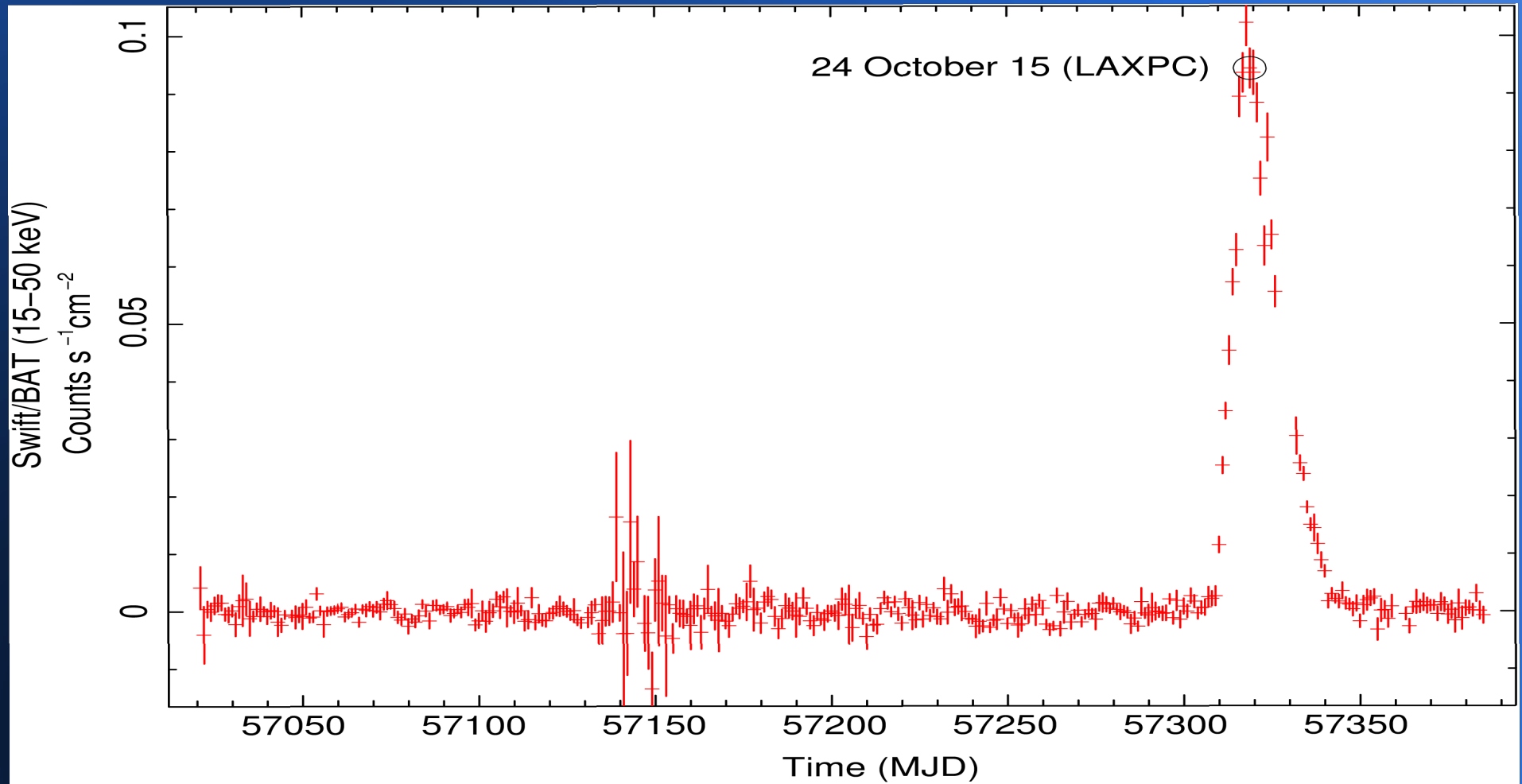
Timing studies of 4U 0115+63 using LAXPC

**LAXPC (Astrosat) detection of the slowest
~1 milli Hz QPO in the Be/X-ray
transient pulsar 4U 0115+63**

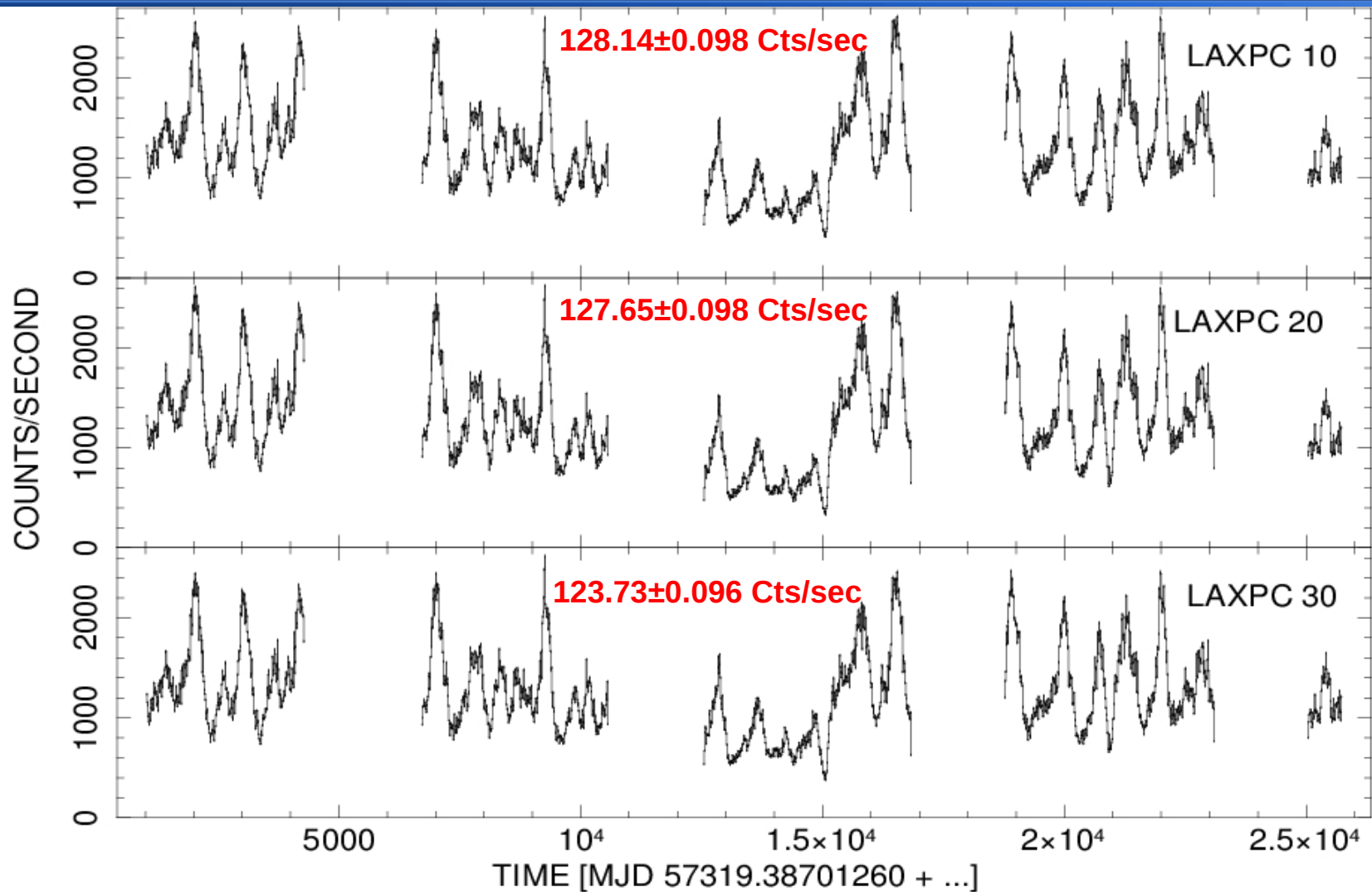
4U 0115+63 RXTE/PCA OUTBURST



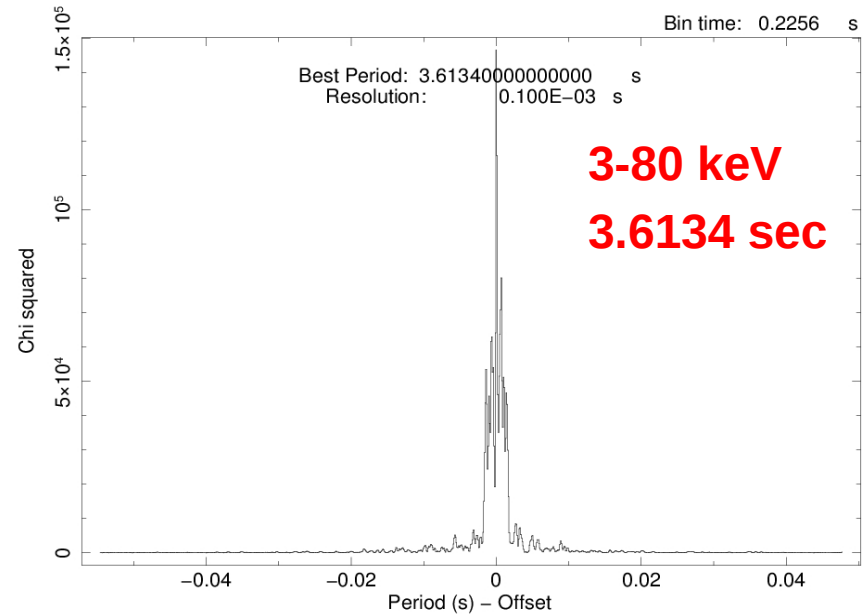
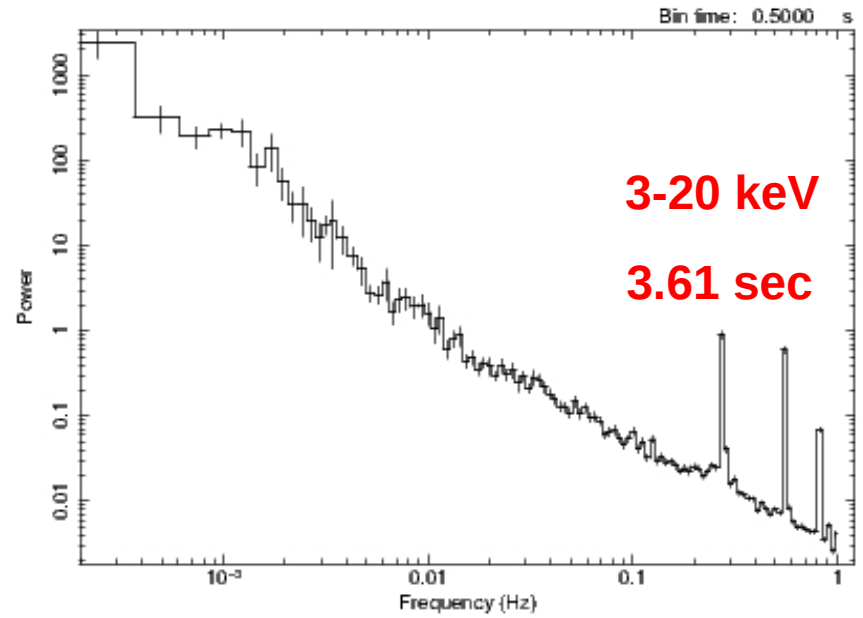
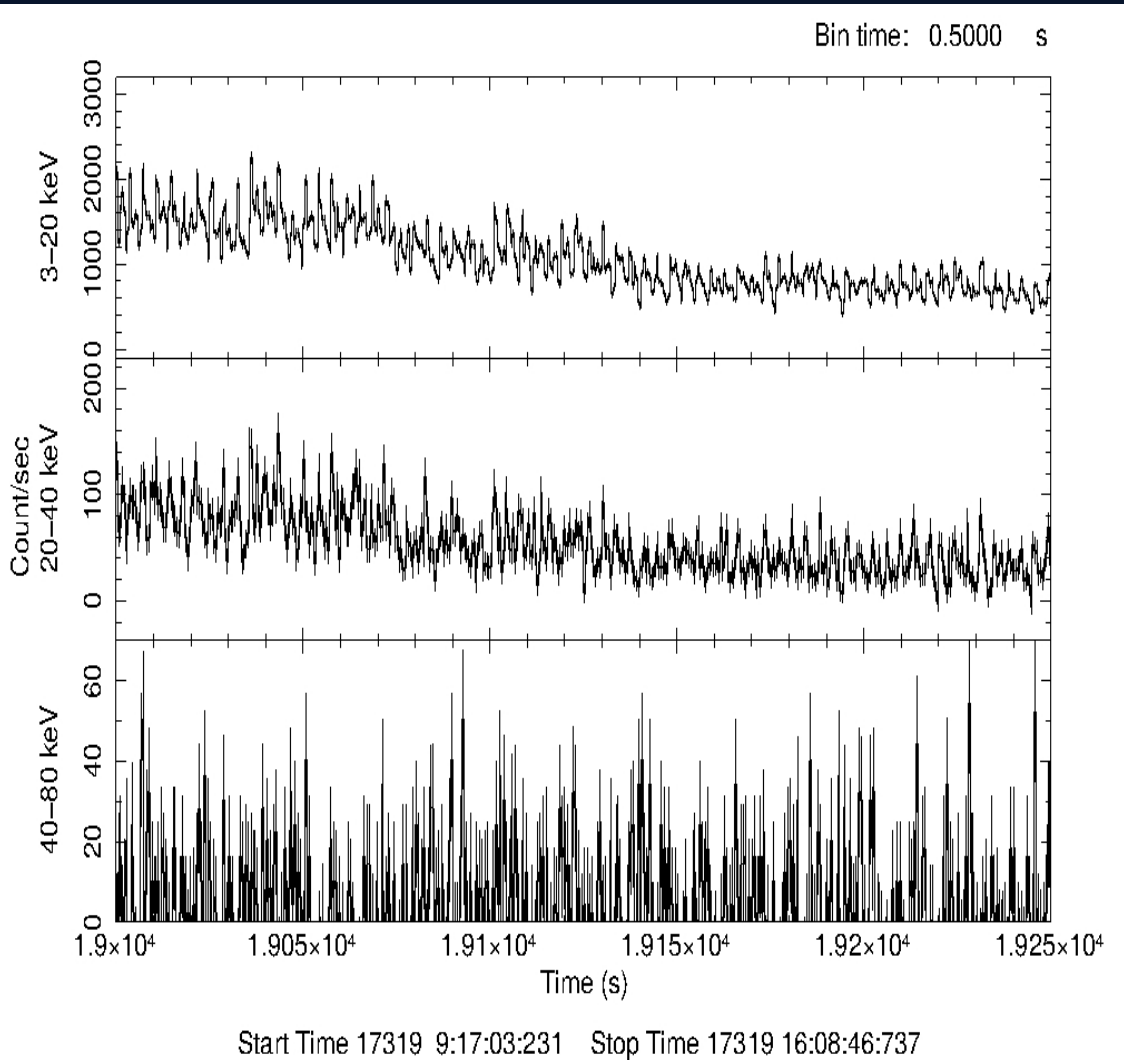
LAXPC observation during brightest 2015 outburst indicated in SWIFT/BAT light curve



LAXPC 10, 20 & 30 lightcurves (3-80 keV)

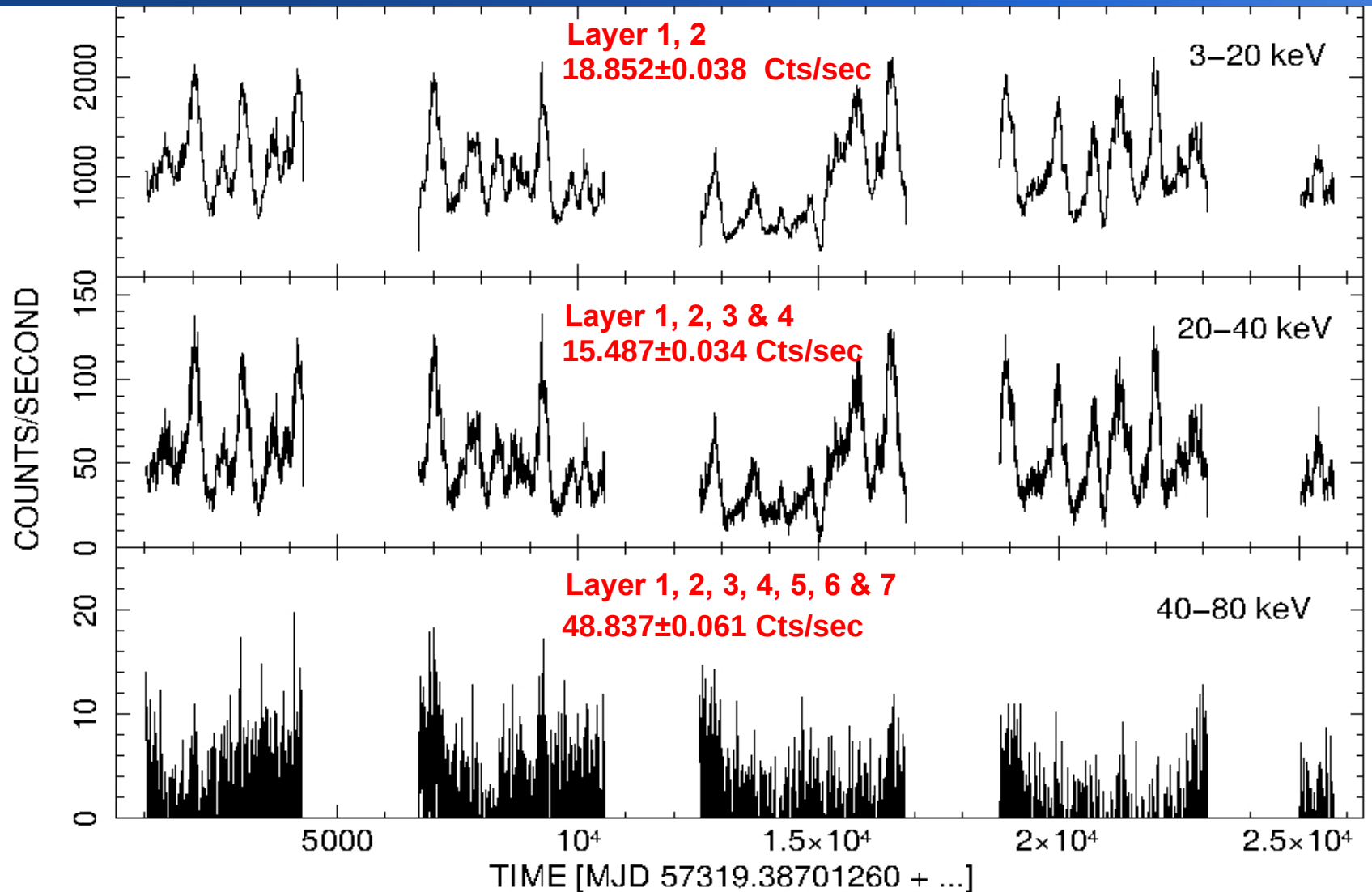


3.61 second pulsation LAXPC 10

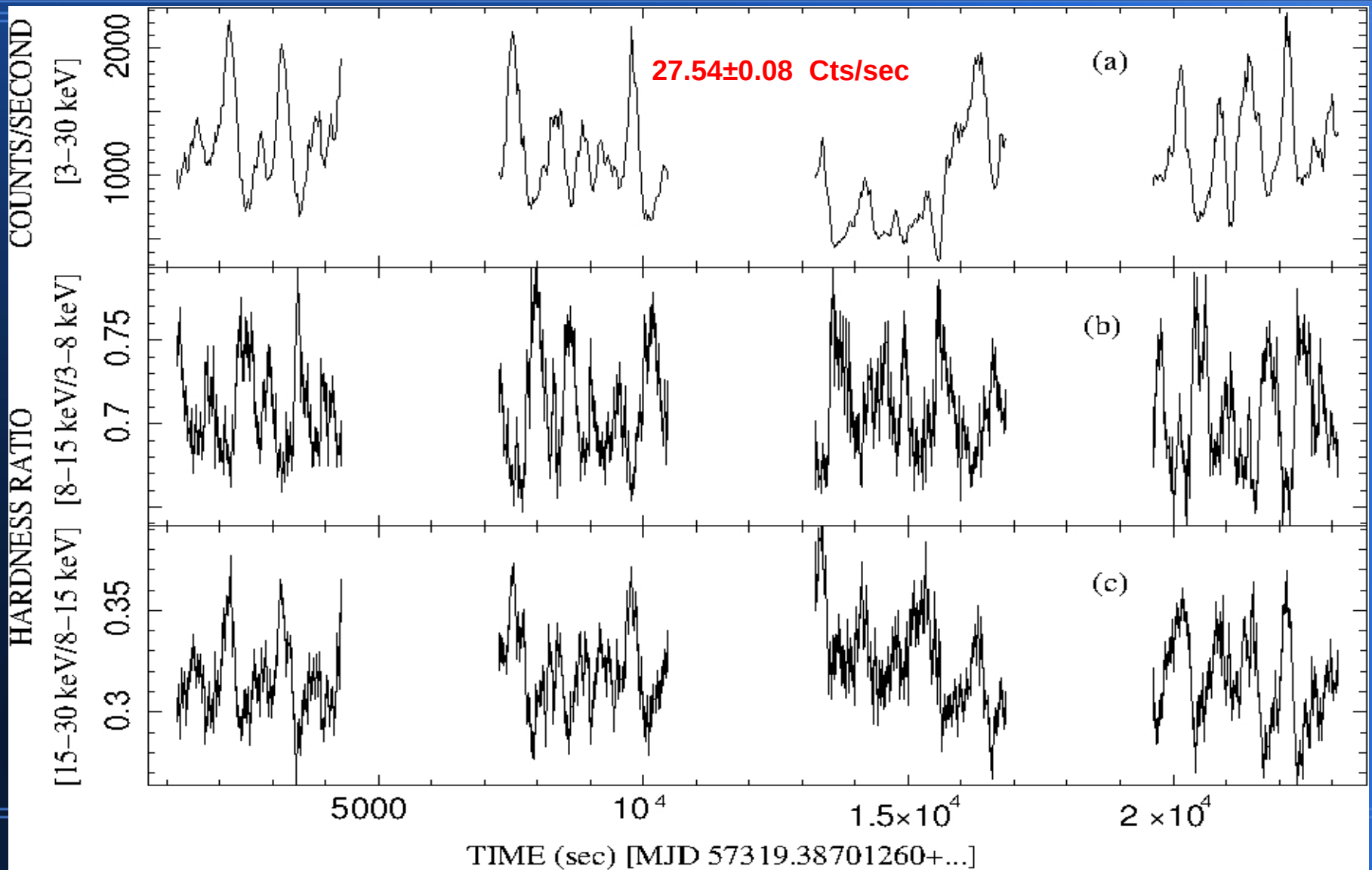


Start Time 17319 9:19:42:615 Stop Time 17319 15:24:55:251

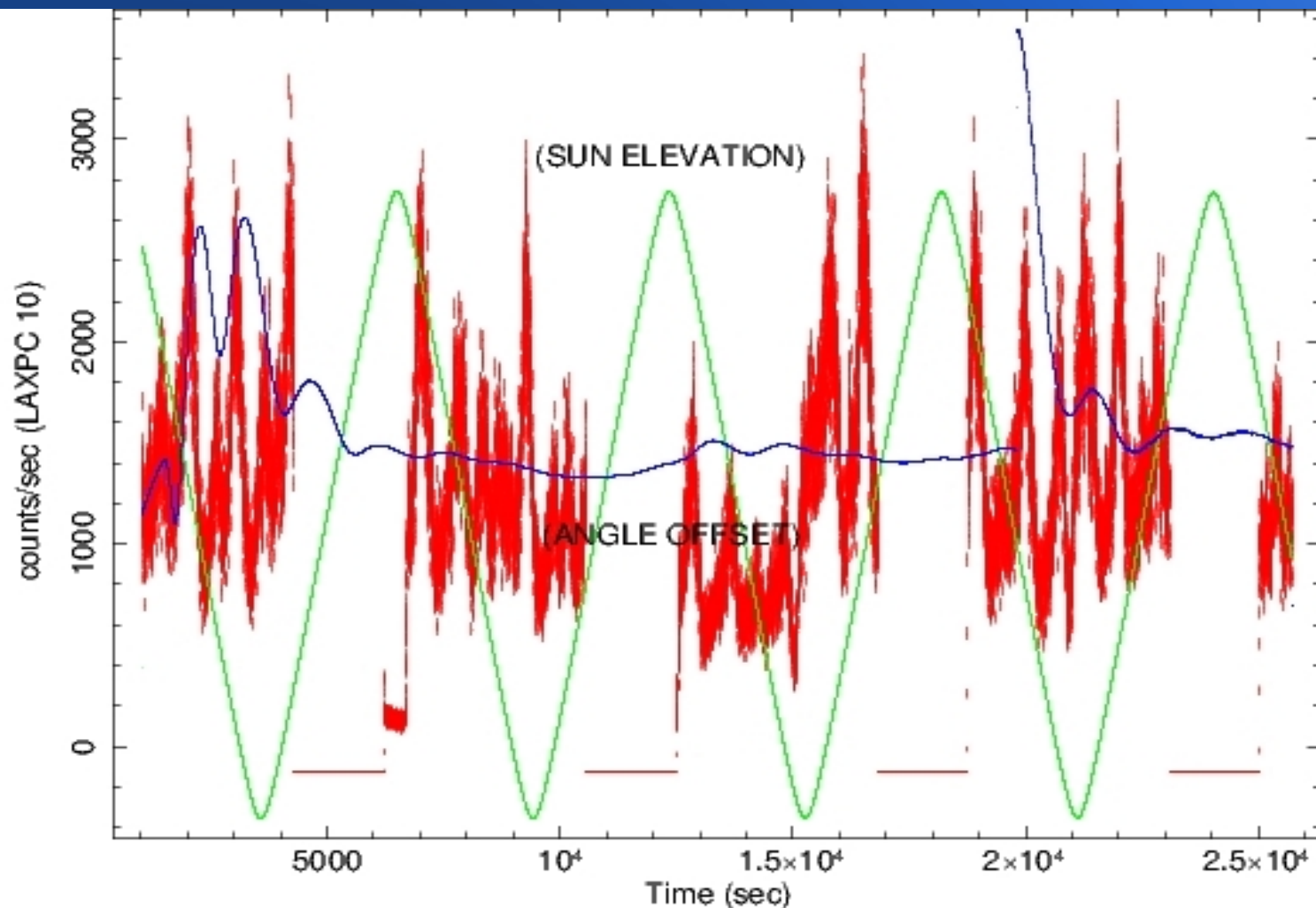
LAXPC 10 energy dependent light curve 3-20, 20-40 & 40-80 keV



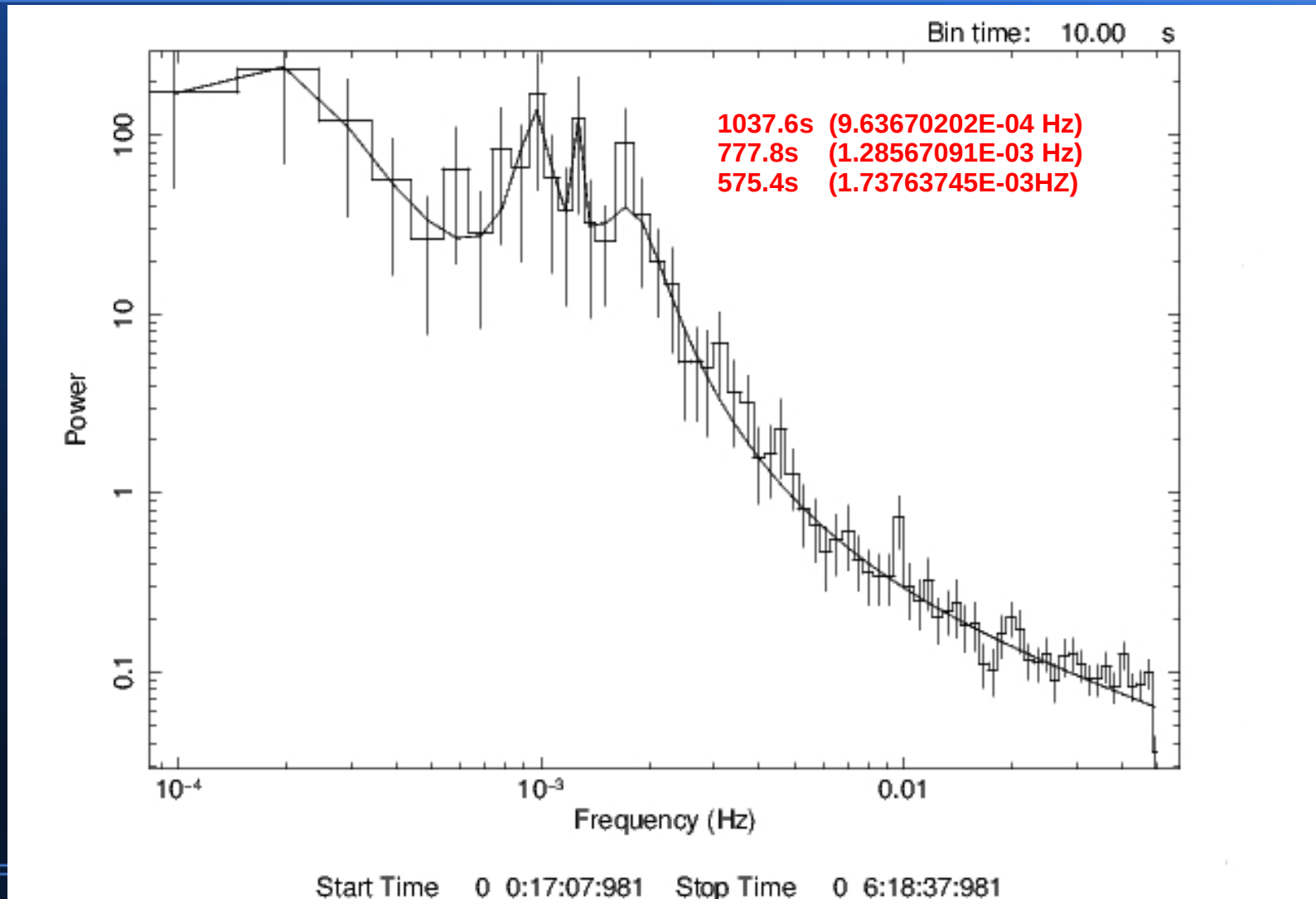
LAXPC 10 : 3-30 keV light curve, HR 1 & HR 2



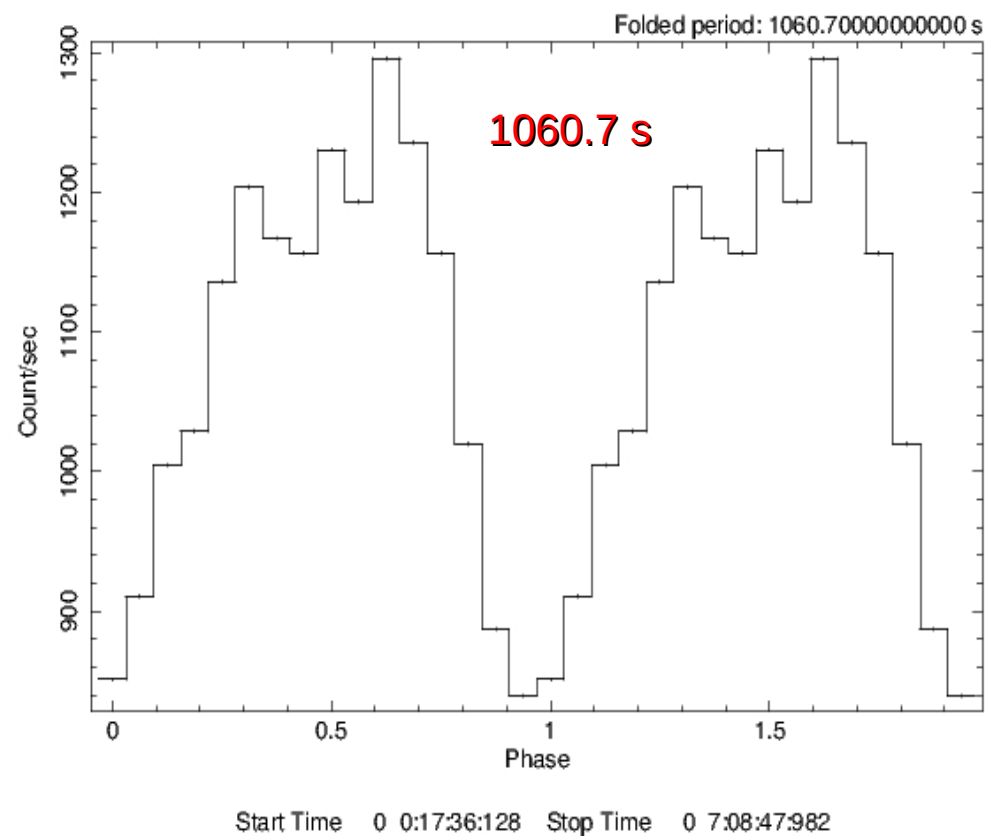
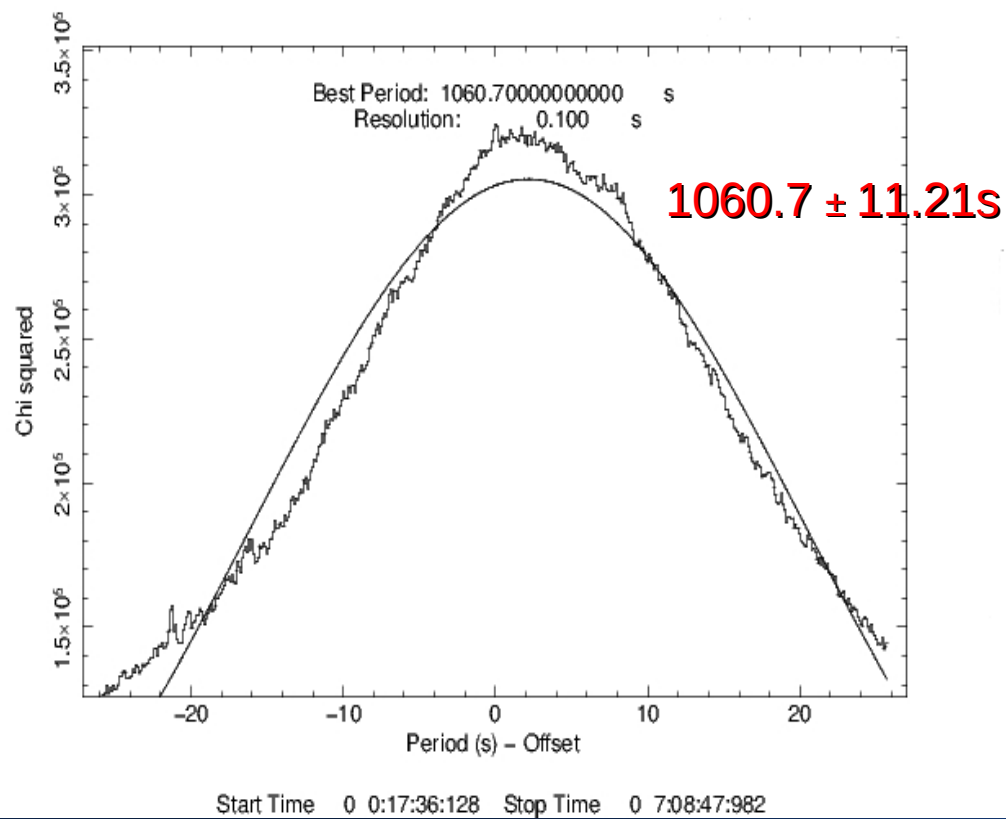
We have observed ~600 sec and 1000 sec quasi periodic oscillations from all three LAXPC 10, 20 and 30. Thus we have cross checked the data for possible fluctuations due to sun elevation angle, angle offset



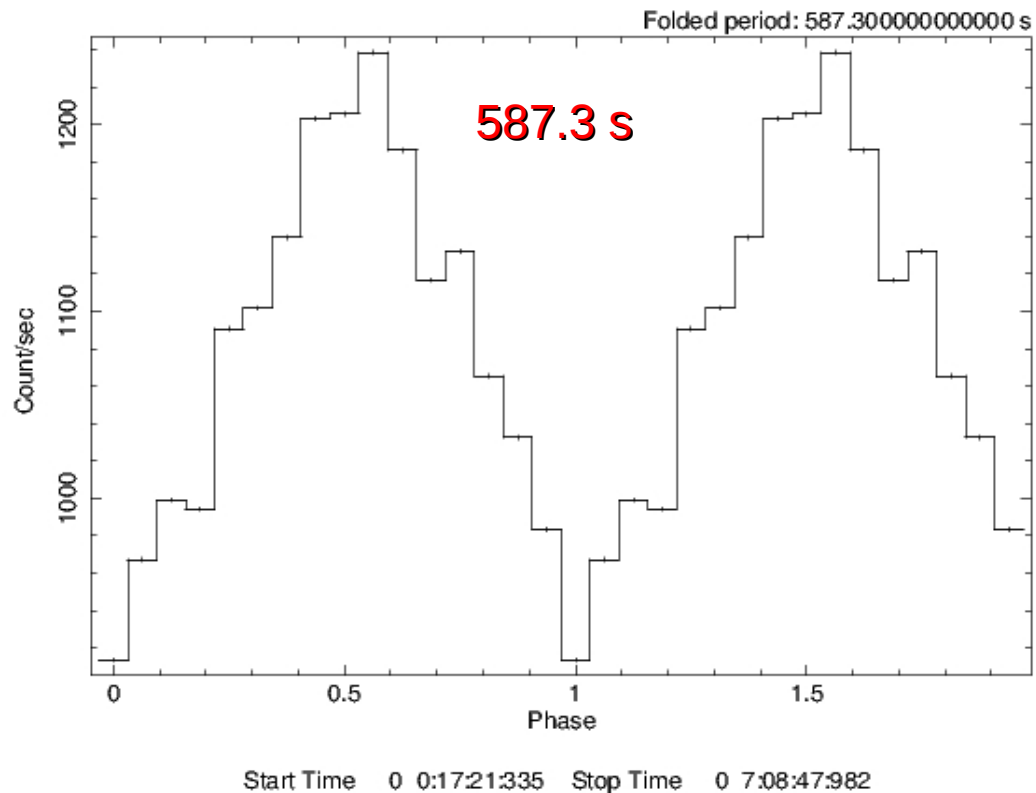
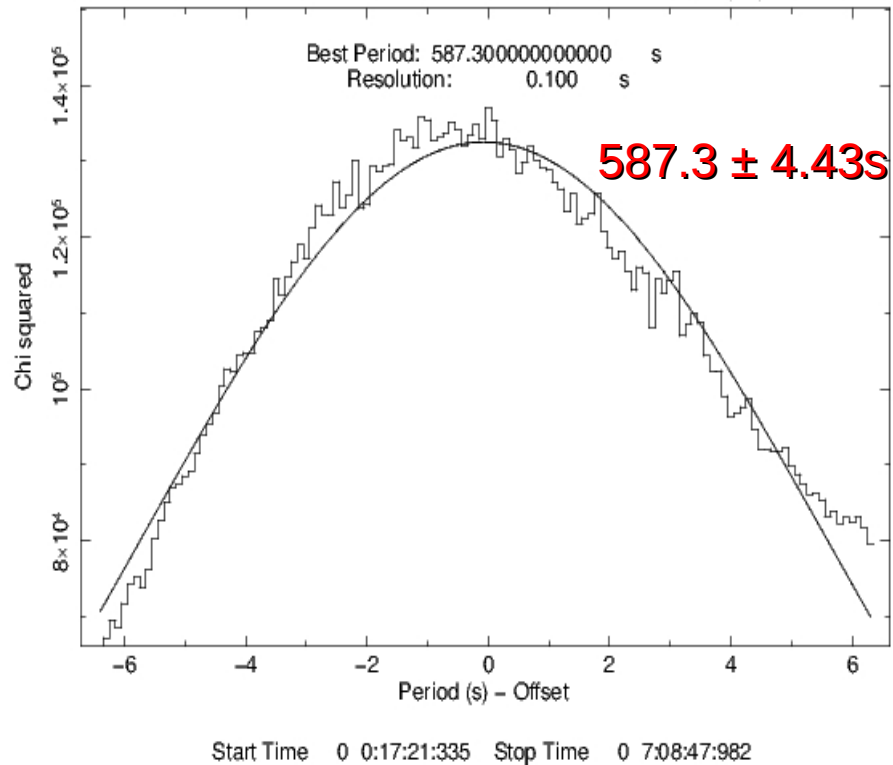
LAXPC 10 : Power Density Spectra of 4U 0115+63 (3-40 keV)



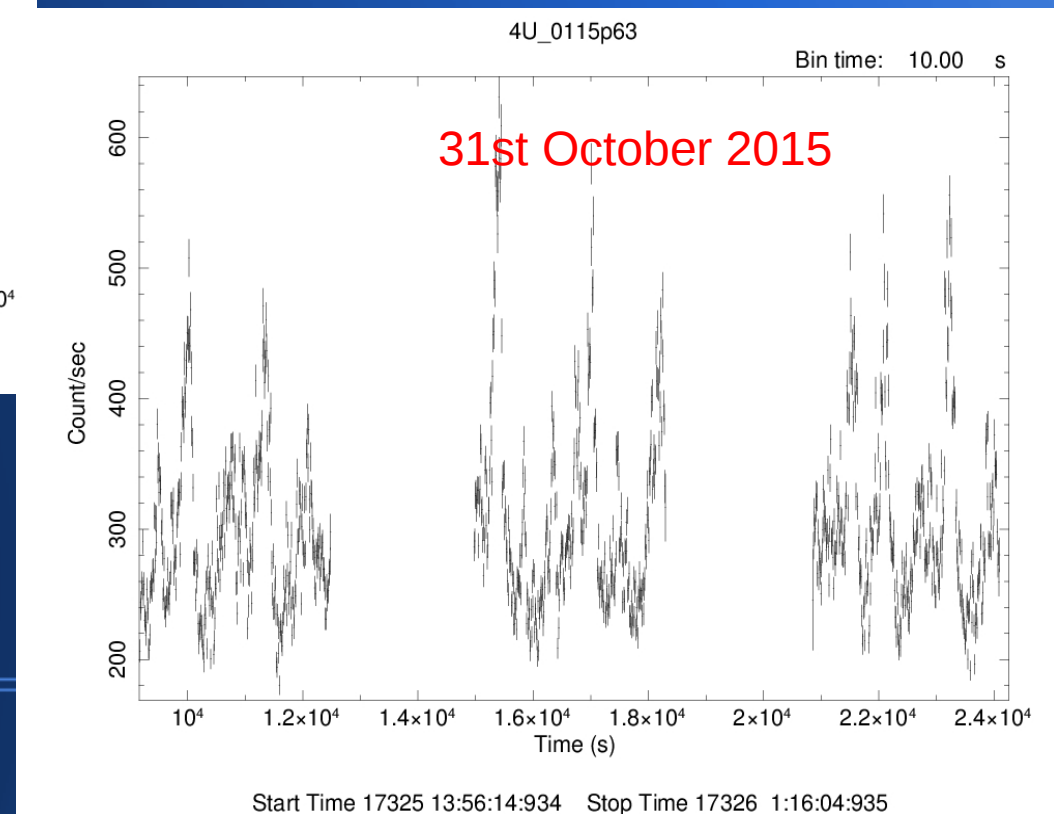
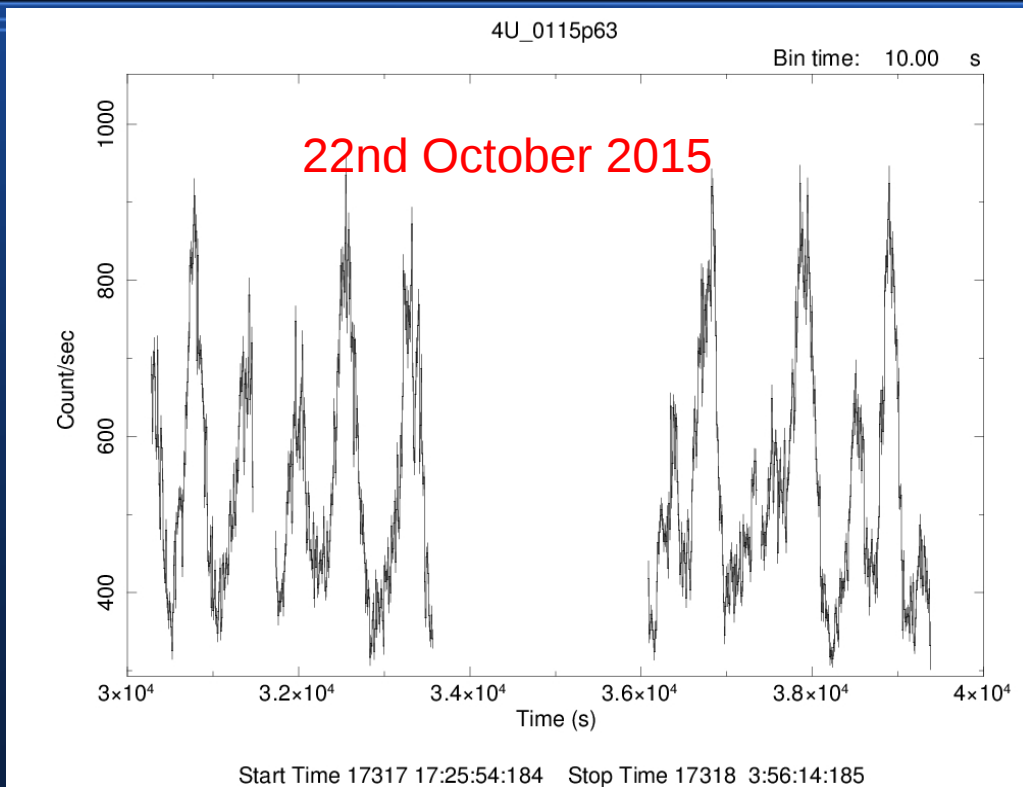
LAXPC 10: Efolded lightcurve



LAXPC 10: Efolded lightcurve



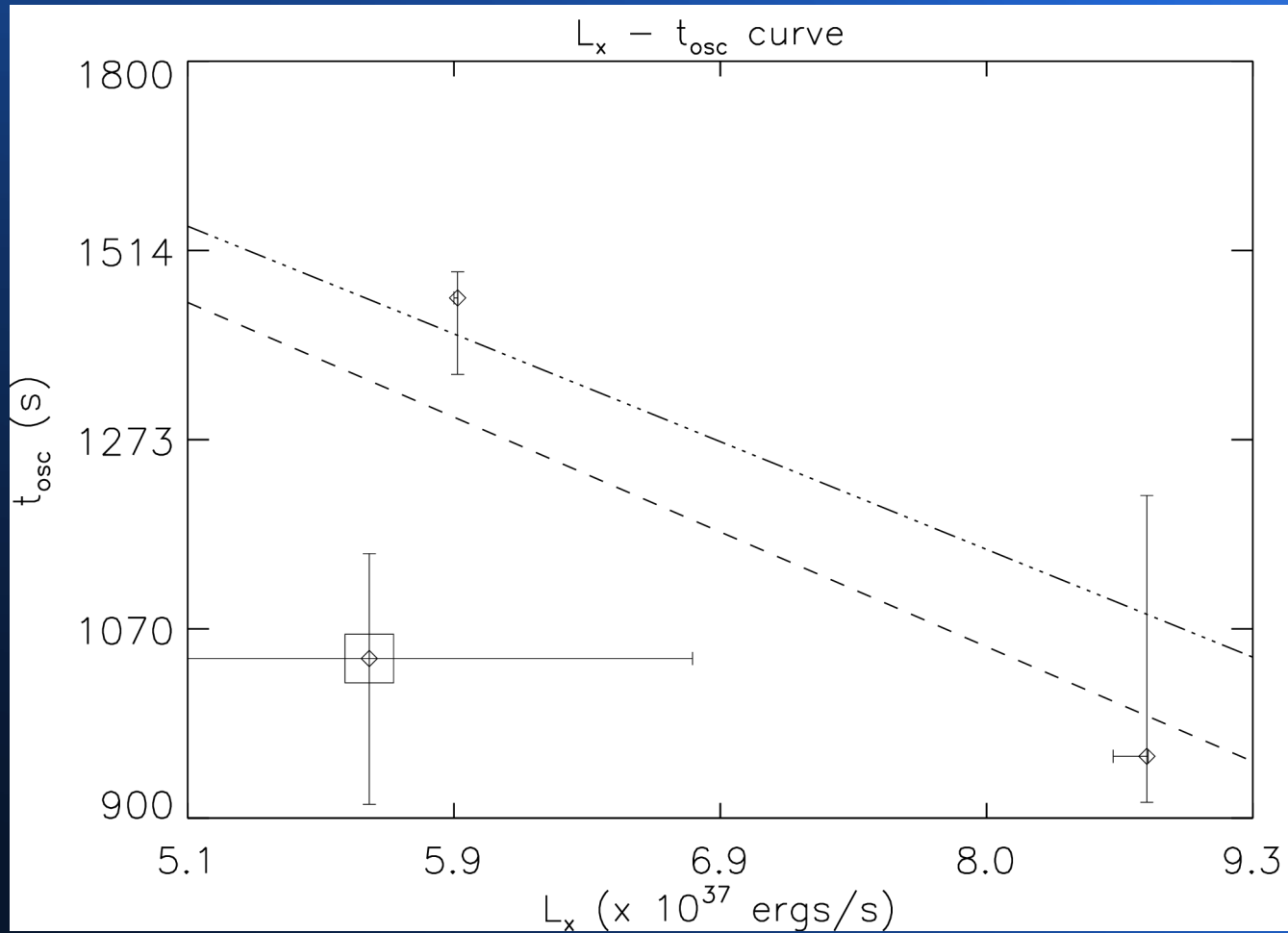
Nustar light curves shows ~600 & 1000 sec oscillations



Comparing results with nustar 2015 outburst of 4U 0115+63

Detector Date	QPO (Hz) in 3-40 keV, Timescales (sec)	RMS (%)	Q-FACTOR	FLUX (3-80 keV) ergs/cm ² /s
NUSTAR	1.04E-03 (9.60E-04 1.18E-03) 954, (1042, 847)	15.6	5.7	1.6343e-08 (1.100e-09 – 3.989e-09) (Luminosity: 9.5816e+37 erg/s)
22-10-15	1.67E-03 (1.64E-03 1.83E-03) 598, (609, 545)	15.8	12.5	
LAXPC10	9.63E-04, (6.78E-04 1.32E-03) 1038, (1474, 756)	29.4	5.3	1.2724e-08 (2.298e-09–7.427e-09) (Luminosity 7.4599e+37 erg/s)
24-10-15	1.73E-03, (1.29E-03 2.035E-03) 575, (774, 492)	19.7	2.4	
NUSTAR	6.92E-04 (6.43E-04 8.29E-04) 1444, (1555, 1206)	9.8	4.2	1.1037e-08(3.310e-09 – 1.185e-08) (Luminosity 6.4708e+37 erg/s)
31-10-15	1.41E-03 (1.28E-03 1.53E-03) 709 (777, 650)	10.7	3.4	

Oscillations and luminosity levels, as observed in the 2015 outburst of 4U 0115+634 in 3-40 keV.



Orbital phase of detected and newly reported QPOs

Year of outburst	Instrument	Observation Id	MJD	Detected QPO (seconds)	Phase
1999	RXTE (PCA)	40411-01-09-00	51248.370825	500 Heindl et al. (1999)	0.973
2004	RXTE (PCA)	90089-01-03-01	53260.170915	511	0.704
2008	RXTE (PCA)	93032-01-03-03	54559.07933	682, 1219	0.119
2011	RXTE (PCA)	96032-01-02-01	55739.57478	683	0.664
2011	RXTE (PCA)	96032-01-03-00	55743.906815	515	0.843
2015	NUSTAR	90102016002	57317.560875	598, 954	0.556
2015	LAXPC (1,2,3)	9000000064	57319.52979	575, 1038	0.637
2015	NUSTAR	90102016004	57325.657985	709, 1444	0.888

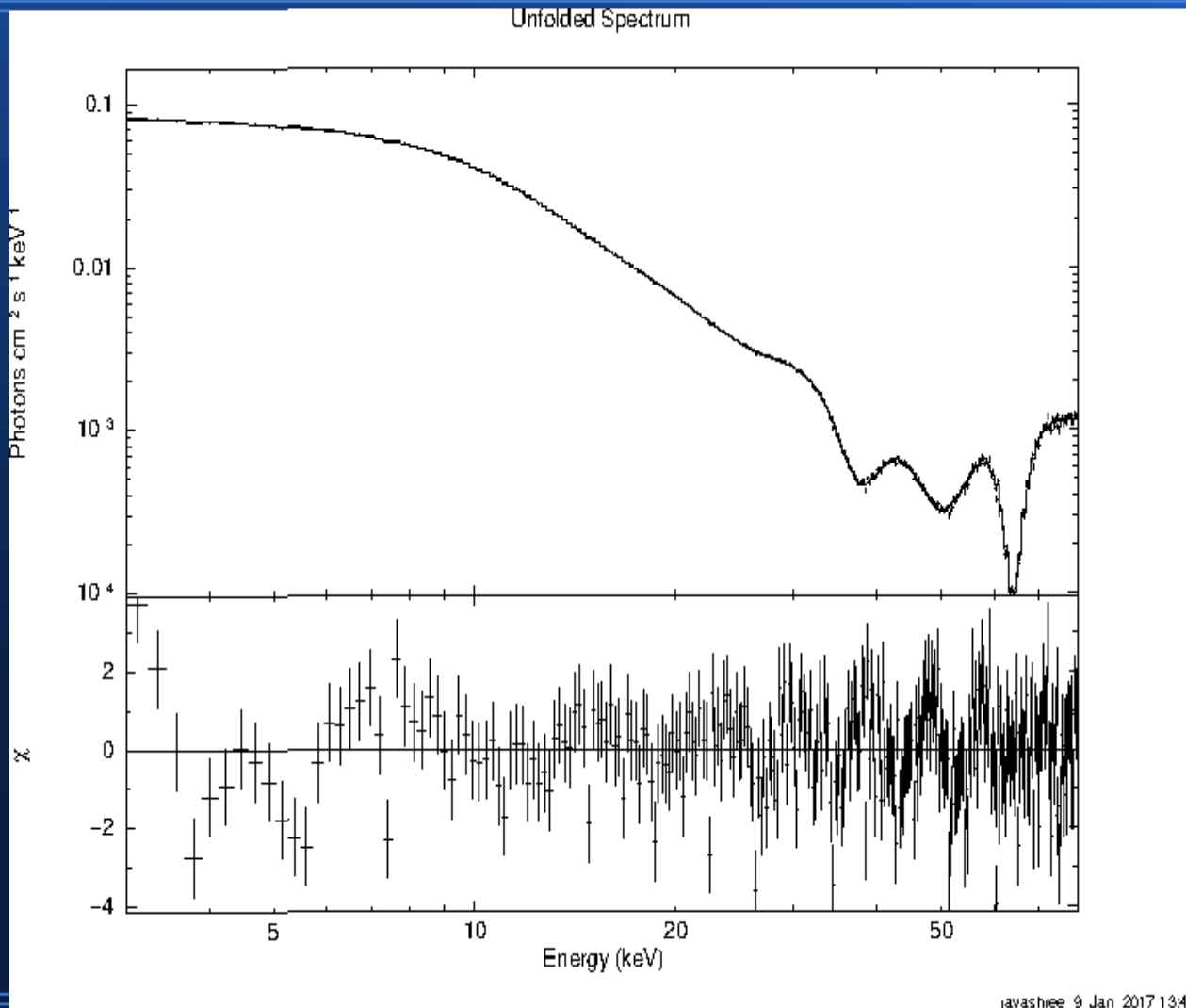
Orbital phase were calculated from periastron passage time (T_w) = 53243.038 from the 2004 outburst of the source and P_{orb} = 24.3174 days (Raichur & Paul 2010).

Table 2: Summary of the characteristics of the QPO 1mHz and 2mHz in the three energy bands.

MJD 57319 corresponds to the date 2015-10-24.

Detector	Energy Range (keV)	QPO 1mHz			QPO 2mHz		
		Frequency ($\times 10^{-4}$ Hz)	RMS %	Quality Factor	Frequency ($\times 10^{-3}$ Hz)	RMS %	Quality Factor
LAXPC 1	3-15	$9.6^{+2.5}_{-4.4}$	19.0	3.5	$1.7^{+0.5}_{-0.36}$	18.6	2.3
	15-30	$9.7^{+1.7}_{-3.9}$	19.0	3.8	$1.7^{+0.5}_{-0.24}$	19.6	5.4
	30-50	$9.8^{+1.0}_{-5.8}$	4.5	6.7	$1.7^{+0.4}_{-0.14}$	5.2	6.2
LAXPC 2	3-15	$9.5^{+3.0}_{-4.9}$	18.9	3.9	$1.7^{+0.6}_{-0.37}$	19.0	2.1
	15-30	$9.7^{+1.7}_{-1.9}$	20.1	3.8	$1.7^{+0.5}_{-0.26}$	20.6	5.5
	30-50	$9.7^{+1.6}_{-0.5}$	6.6	5.9	$1.7^{+0.3}_{-0.18}$	7.4	5.8
LAXPC 3	3-15	$9.6^{+2.7}_{-3.2}$	19.2	2.8	$1.8^{+0.6}_{-0.63}$	17.7	2.4
	15-30	$9.8^{+1.8}_{-3.1}$	18.9	3.3	$1.7^{+0.3}_{-0.25}$	19.7	5.6
	30-50	$10.0^{+1.1}_{-2.8}$	4.6	5.3	$1.8^{+0.1}_{-0.22}$	4.6	7.2

Spectral Study of LAXPC 10 (3-80 keV)



Model $Tbabs^* powerlaw^* highecut$
 $cyclabs^* cyclabs^* cyclabs^* cyclabs^* cyc$
 $labs$

Powerlaw Photon Index : 0.37 (-0.03, 0.03)

Reduced chi sq: 1.48 (405.23 for 272 dof)

Flux $1.2724e-08$ ergs/cm²/s ($1.255e-08$ - $1.283e-08$), Luminosity at 7kpc; $7.4599e+37$ ergs/s

Cut off energy : 8.5 (-0.43, 0.50) keV

Fold energy : 34.3 (-2.58, 4.69) keV

CYCLOTRON LINE ENERGIES & HARMONICS

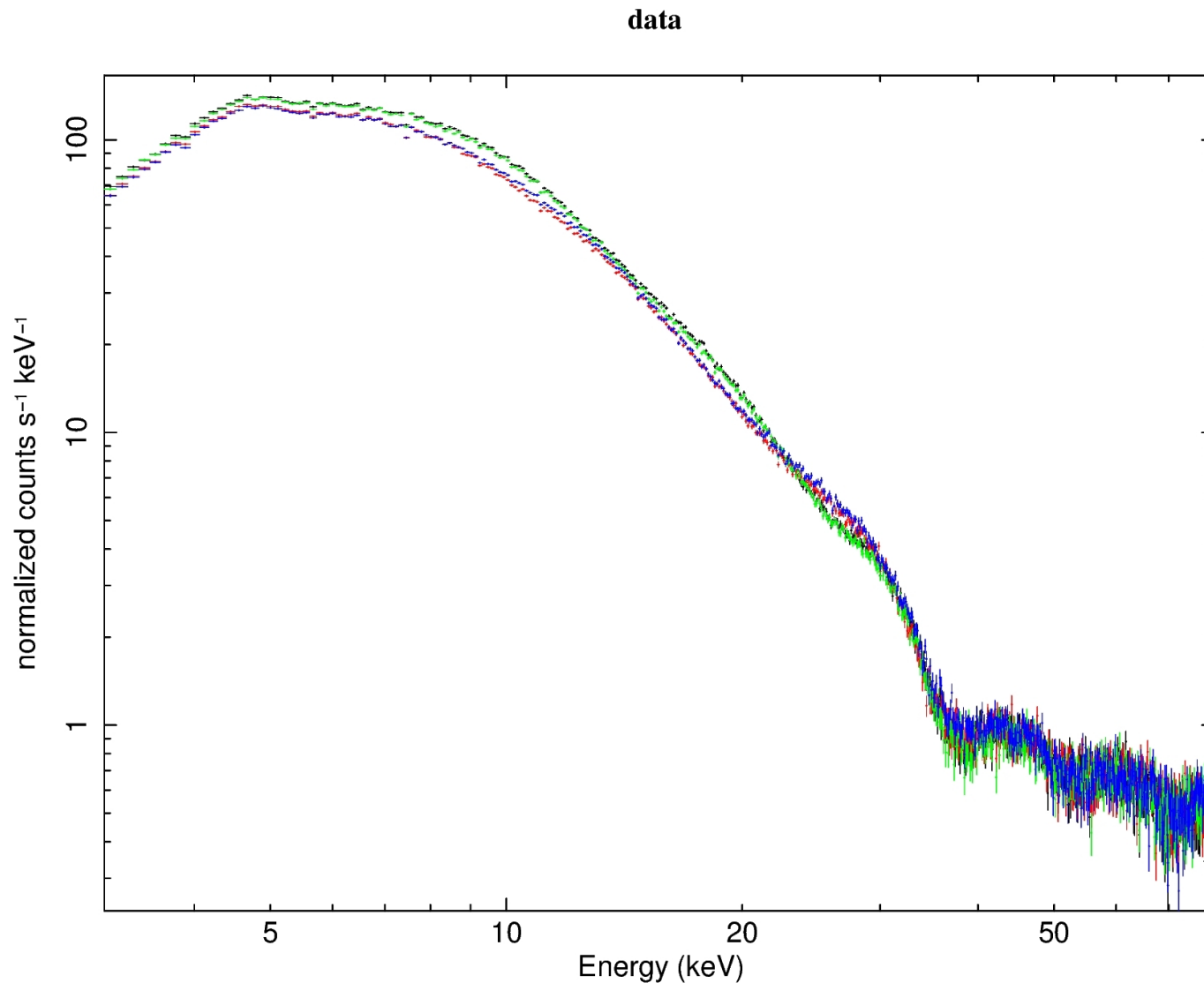
13.5 keV, 23.2 keV, 37.3 keV, 49.1 keV, 63.9 keV

Cyclotron line parameters

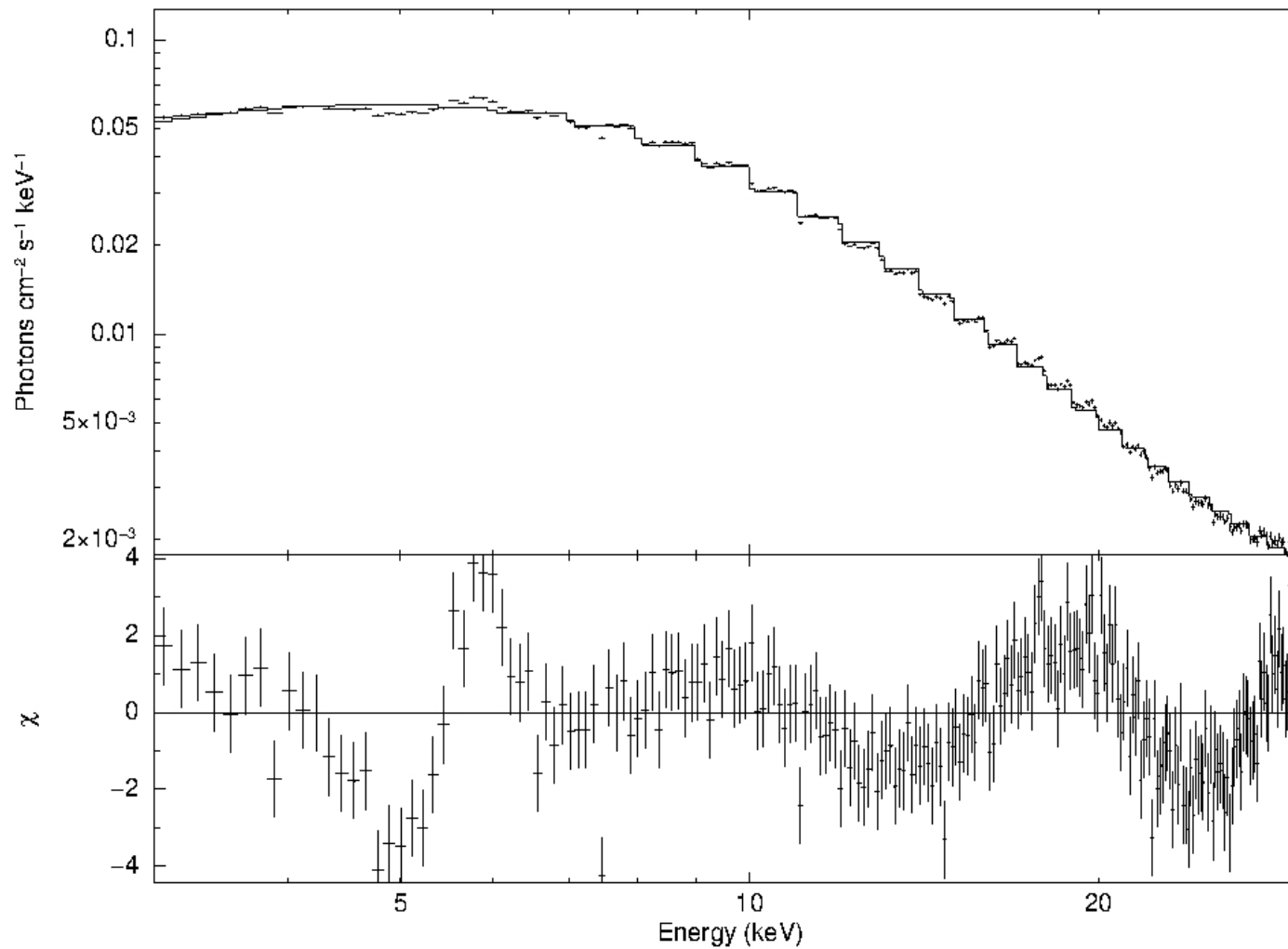
Cyclotron line Energy (keV)	Width (keV)	Depth
13.5 (-0.29, 0.26)	7.40 (-1.01, 1.12)	0.71(-0.1, 0.11)
23.2 (-1.11, 0.84)	4.48 (-0.76, 0.76)	1.83(-0.21, 0.18)
37.3 (-0.29, 0.25)	9.39 (-1.34, 1.40)	1.12(-0.15, 0.13)
49.1 (-0.71, 0.56)	7.38 (-1.54, 1.89)	2.07(-0.10, 0.14)
63.9 (-0.53, 0.61)	2.56 (-2.55, 2.00)	2.73 (-0.67, 5.84)

Pulse Phase Resolved Spectroscopy

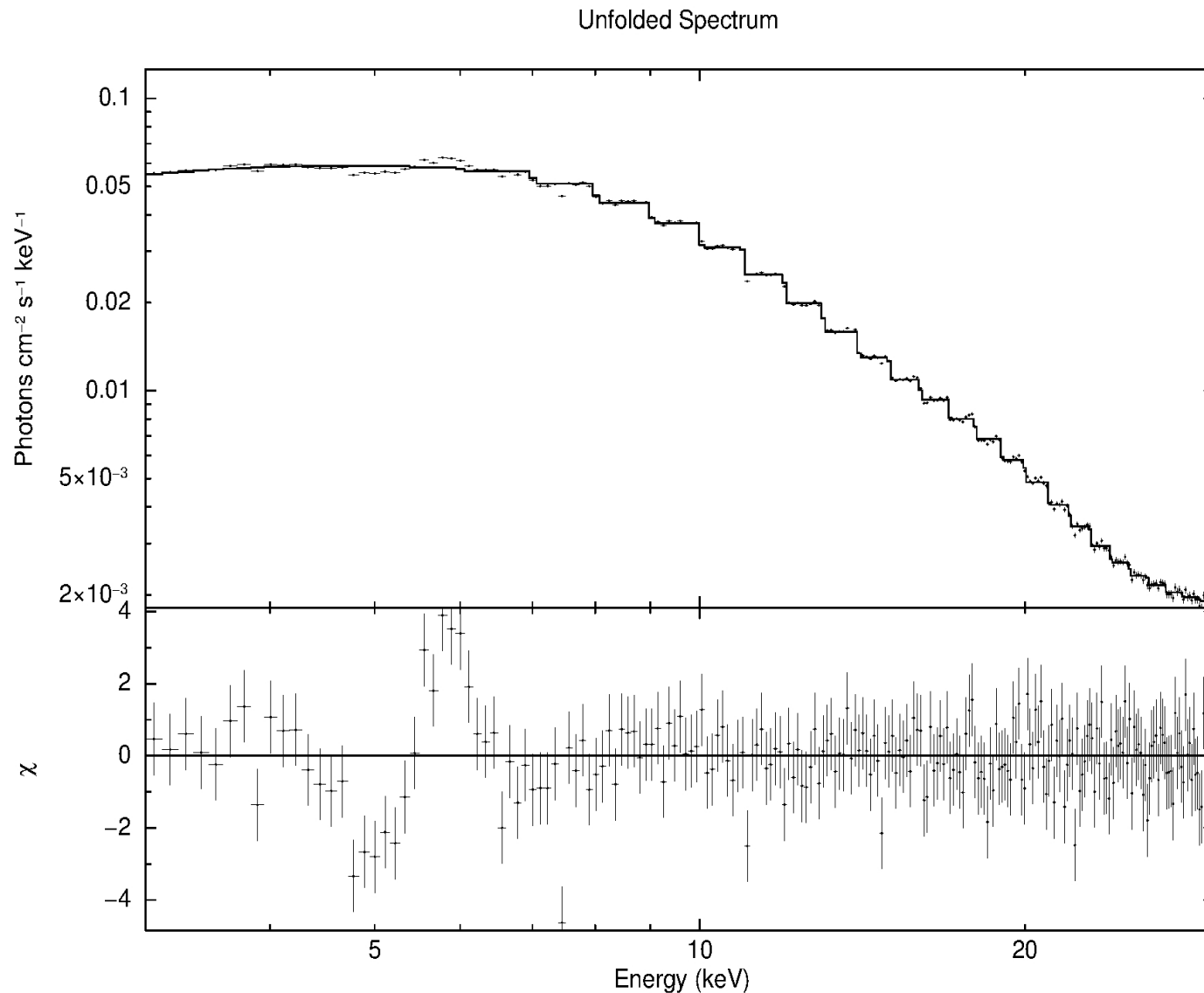
Phase wise spectra of LAXPC 1: (Black:0-0.25, Red:0.25-0.5, Green:0.5-0.75, Blue:0.75-1)



Without Cyclotron line continuum spectra (3-30 keV) of LAXPC 1 from 0.0-0.25 phase



Spectra (3-30 keV) of LAXPC 1 from 0.0-0.25 phase



Pulse phase resolve spectroscopy parameters (3-30 keV) of LAXPC 1

Model	Parameters	LAXPC 1 Phase			
		0.0-0.25	0.25-0.5	0.5-0.75	0.75-1
Power Law	PhoIndex Γ	$0.08^{0.03}_{-0.03}$	$0.05^{0.06}_{-0.11}$	$0.08^{0.05}_{-0.05}$	$0.09^{0.05}_{-0.09}$
Highecut	cutoffE E_c (keV)	$6.85^{0.19}_{-0.22}$	$6.97^{0.25}_{-0.38}$	$6.79^{0.27}_{-0.31}$	$6.79^{0.29}_{-0.32}$
	foldE E_f (keV)	$12.03^{2.28}_{-1.36}$	$9.28^{1.37}_{-0.50}$	$10.11^{2.39}_{-1.14}$	$9.36^{0.84}_{-0.44}$
cyclabs 1	Depth D_f (τ)	$0.56^{0.04}_{-0.04}$	$0.32^{0.11}_{-0.11}$	$0.56^{0.08}_{-0.05}$	$0.23^{0.25}_{-0.15}$
	Energy E_{cycl} (keV)	$13.41^{0.23}_{-0.25}$	$10.35^{0.76}_{-1.47}$	$13.87^{0.36}_{-0.43}$	$11.20^{2.11}_{-2.80}$
	Width W_f (keV)	$5.67^{0.45}_{-0.41}$	$6.58^{3.91}_{-2.85}$	$5.62^{0.79}_{-0.67}$	$6.80^{3.97}_{-4.53}$
cyclabs 2	Depth D_f (τ)	$1.13^{0.22}_{-0.17}$	$0.71^{0.21}_{-0.27}$	$0.84^{0.31}_{-0.20}$	$0.66^{0.20}_{-0.36}$
	Energy E_{cycl} (keV)	$22.89^{0.36}_{-0.39}$	$19.20^{1.27}_{-1.79}$	$23.45^{0.58}_{-0.67}$	$18.55^{1.67}_{-1.65}$
	Width W_f (keV)	$5.37^{1.19}_{-1.08}$	$7.49^{1.76}_{-1.71}$	$7.64^{2.08}_{-1.72}$	$7.29^{1.57}_{-2.27}$
Flux (3-30 keV)	$\times 10^{-9}$ ergcm $^{-2}$ s $^{-1}$	$7.87^{0.01}_{-0.22}$	$7.23^{0.03}_{-0.72}$	$7.79^{0.01}_{-0.17}$	$7.37^{0.04}_{-1.06}$
reduced χ^2		1.14	1.11	1.08	1.19

Thank you

Sources which shows QPO less than spin frequency

4U 1901+03, the QPO is detected at ~ 0.135 Hz (James et al 2010).

In the Beat Frequency Model, the expected QPO frequency range, for source luminosity between $5.8 \times 10^{37} \text{ erg s}^{-1}$ at the peak of the outburst and $0.16 \times 10^{37} \text{ erg s}^{-1}$ when the QPOs are detected, is 2.05 to 0.135 Hz.

Cen X-3, 4U 0115+63, 4U 1626-67, Her X-1, LMC X-4, V0332+52, SMC X-1 and KS 1947+300, the pulsar frequency is higher than the QPO frequency hence the Keplerian frequency model is inapplicable. It is expected that centrifugal forces inhibit mass accretion if the Keplerian frequency at the inner disk radius is less than the spin frequency of the pulsar.

The Keplerian frequency model (KFM) (van der Klis et al. 1987) and the beat frequency model (BFM) (Alpar & Shaham 1985; Lamb et al. 1985) are popular models in this regard.

Similar kinds of structured variabilities have been observed from a few black hole X-ray binaries like GRS 1915+105 and IGR J17091-3624 in their p variability class which shows a quasi periodic flares in the timescales of 40-120 seconds (Altamirano et al. 2011).

Possible explanations of mHz QPO

1. Viscous relaxation time-scales caused by the thermal disk instabilities can be used for the ~ 1000 and 600 sec oscillations, as the source was at the peak of the outburst when these oscillations were observed (close to Eddington luminosity). Viscous time-scales for HMXB accreting source are given as

$$t_{\text{visc}} = 480 \alpha^{-4/5} \left(\frac{\dot{M}}{10^{17} \text{ g/s}} \right)^{-3/10} \left(\frac{M^*}{M_{\odot}} \right)^{1/4} \left(\frac{R_m}{1000 \text{ km}} \right)^{5/4} \text{ s} \quad (4)$$

Using $Lx \simeq GMM\dot{M}/R^*$, this gives

$$t_{\text{visc}} = 991.1 \left(\frac{Lx}{10^{37} \text{ erg s}^{-1}} \right)^{-23/35} \left(\frac{\alpha}{0.1} \right)^{-109/230} \left(\frac{R^*}{10 \text{ km}} \right)^{39/14} \left(\frac{M^*}{1.4 M_{\odot}} \right)^{-4/7} \text{ s} \quad (5)$$

As seen from the dashed-dot line in Fig. 1, this expression does follow the trend of oscillation time scales with luminosity.

2. Shirakawa & Lai (2002). They reasoned that a warped or precessing accretion disk caused by mis-aligned vectors of the disk angular momentum and the magnetic field can lead to such observational signatures.

$$\nu_{\text{qpo}} \propto M^{0.71}$$

Introduction to 4U 0115+63

The transient X-ray source 4U 0115+63 was first reported from UHURU observations in 1971 (Whitelock et al. 1989).

Binary with an orbital period of 24.3 day and moderate eccentricity of 0.34 (Rappaport et al. 1978) at a distance of 7 kpc. Pulsation period of 3.61 seconds.

A spin up rate of $P = -(7.24 \pm 0.03) \times 10^{-6}$ s/d was observed from the source during 2008 outburst (Jun Li et al. 2012).

Unger et al. (1998) classified the spectral type of optical companion V635 Cas as O9e star which was earlier classified as Be star. Negueruela et al. (2001) found V635 Cas to be a 15th magnitude Be Star of mass $\sim 18 M_{\odot}$ and radius $8 R_{\odot}$.

Whitlock et al. (1989) analyzed the Vela 5B satellite data for 1968 May-1979 June period, during which six outbursts, occurred in the source. They found that 1969 August, 1970 January, 1970 August and 1971 January outburst were separated with a gap of ~ 180 days.

A recurrent time of 2.9-3.5 years between the X-ray outburst from the transient was observed since 1971. Even though X-ray outburst was not detected during 1983-84 but an outburst was observed during 1987 with the Ginga which was predicted on the basis of recurrence period.

Introduction to 4U 0115+63

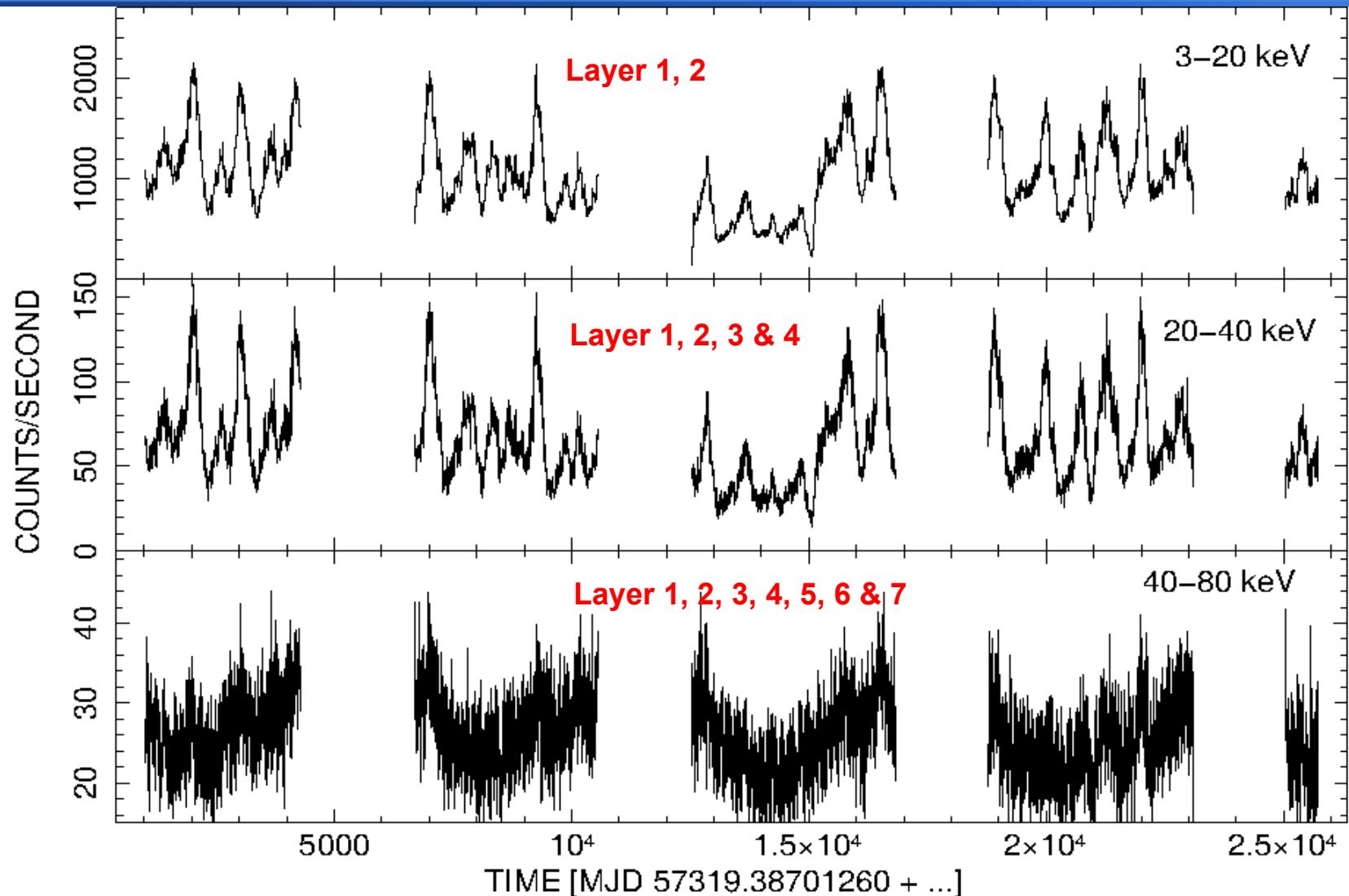
An episodic mass transfer from the companion is suggested as the trigger for the onset of the outburst. The X-ray source undergoes type-II outbursts and several small flares and type-I outbursts. There is indication of ~ 3 -5 year quasi-cyclic intensity variations that may be due to loss and reformation of the shell/disk around the Be star (Negueruela et al. 2001).

White et al. (1983) confirmed the cyclotron line feature in the source. The electron cyclotron lines were found at 11.5 keV and 23 keV. Energy of the fundamental cyclotron line at ~ 11.5 keV leads to the estimation of the magnetic field strength $\sim 1.2 \times 10^{12}$ gauss at the surface of the neutron star.

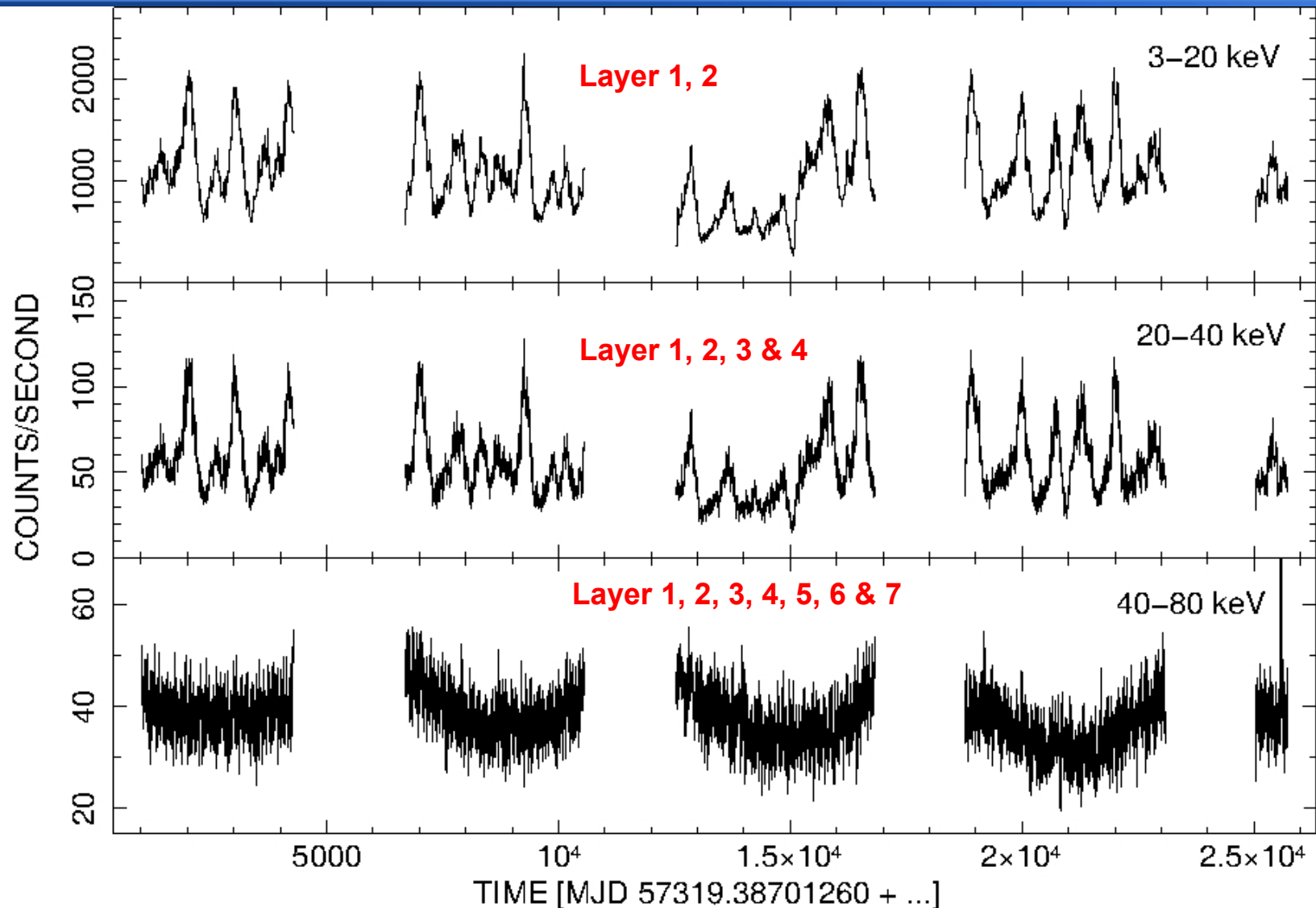
Santangelo et al. (1999) analyzed the BeppoSAX data of 1999 March 19. They clearly detected four cyclotron lines in the energy spectrum of the source. The phase dependent absorption features were present at 12.74, 24.16, 35.74 and 49.5 keV in the ratio 1 : (1.9) : (2.8) : (3.9) with the fundamental centeroid frequency.

Boldin et al. (2013) , 2011 outburst of the source detected 4 harmonics of ~ 11 keV at 24, 35.6, 48.8 and 60.7 keV.

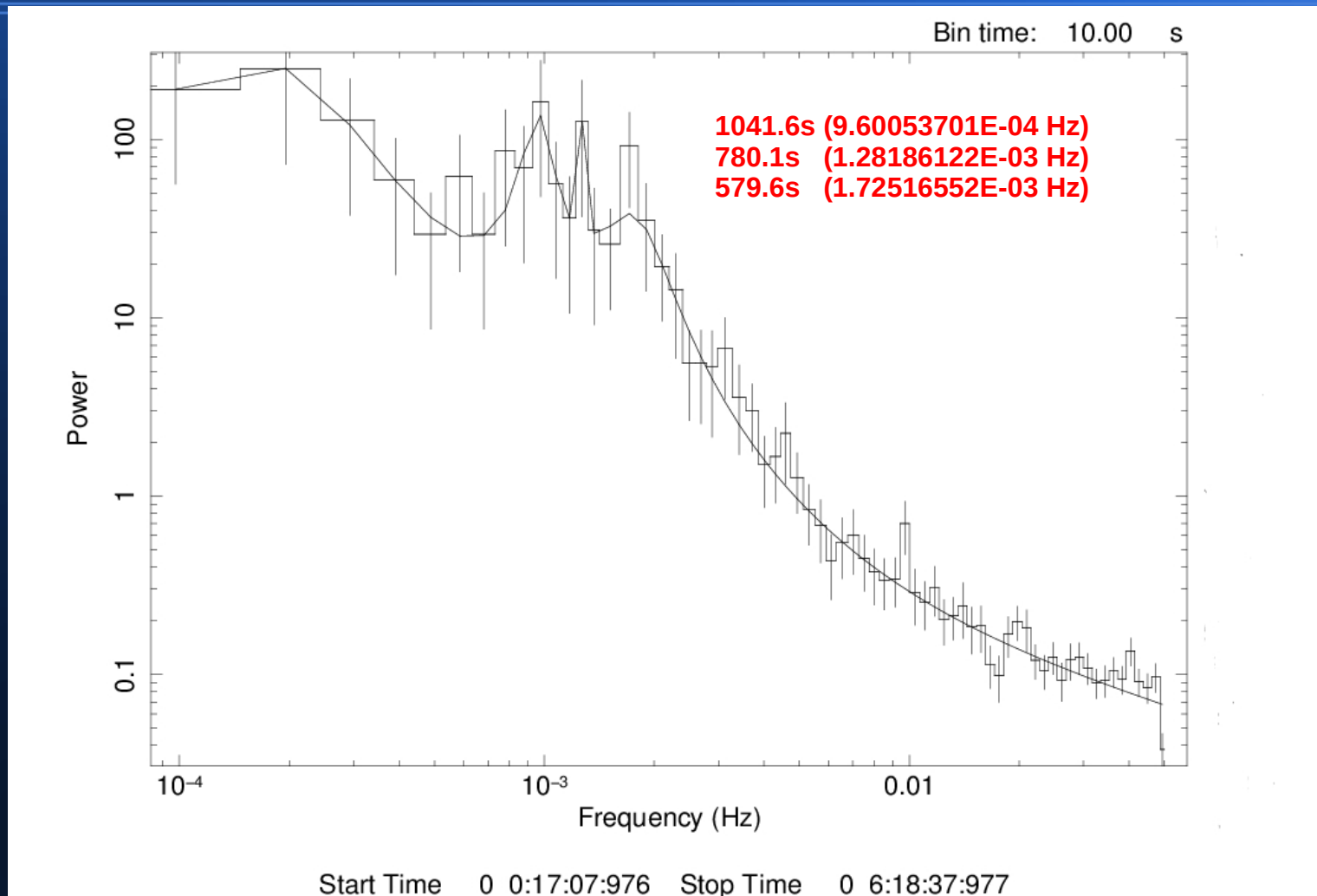
LAXPC 20 energy dependent light curve 3-20, 20-40 & 40-80 keV



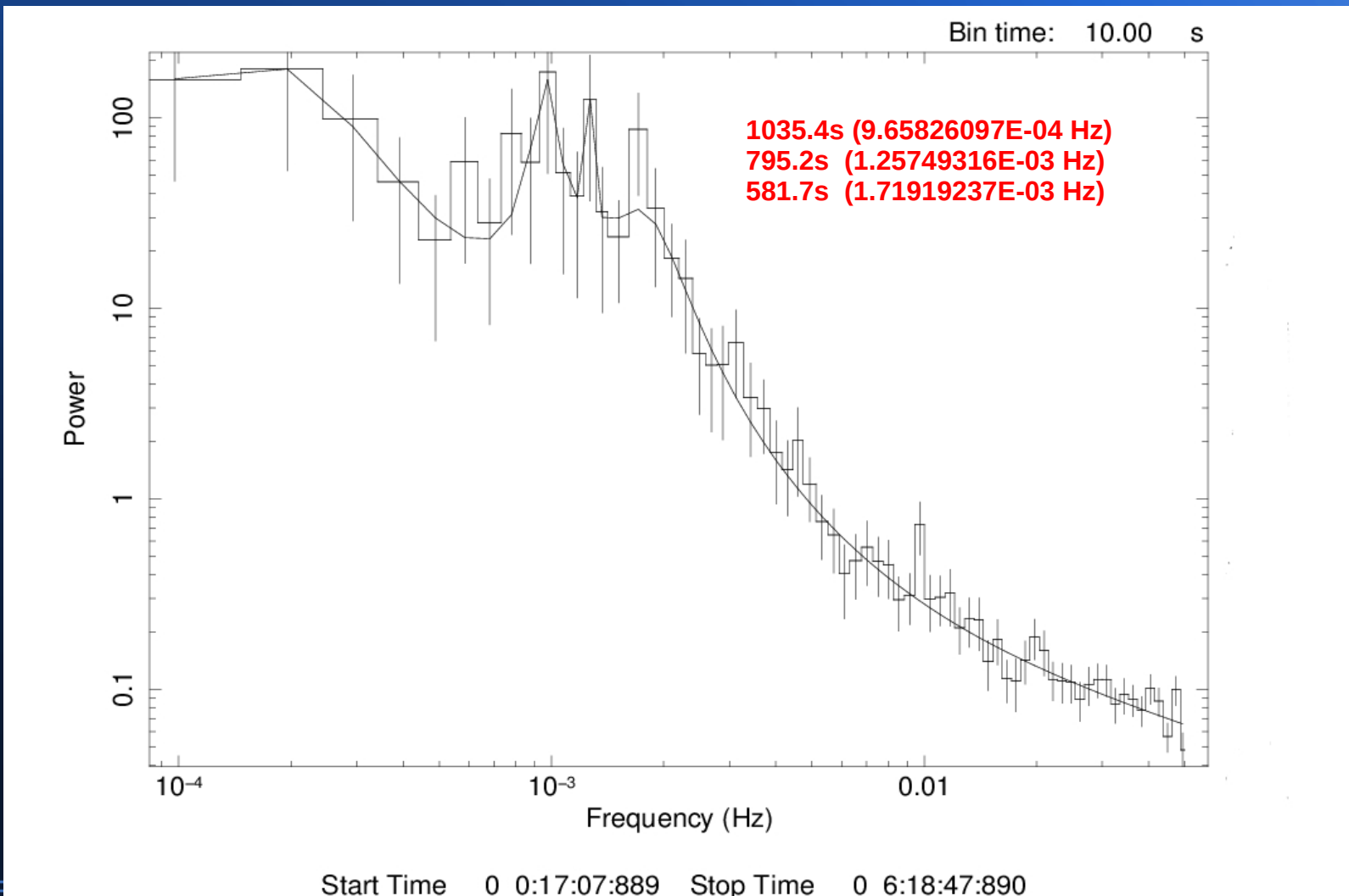
LAXPC 30 energy dependent light curve 3-20, 20-40 & 40-80 keV



LAXPC 20 : Power Density Spectra of 4U 0115+63 (3-40 keV)



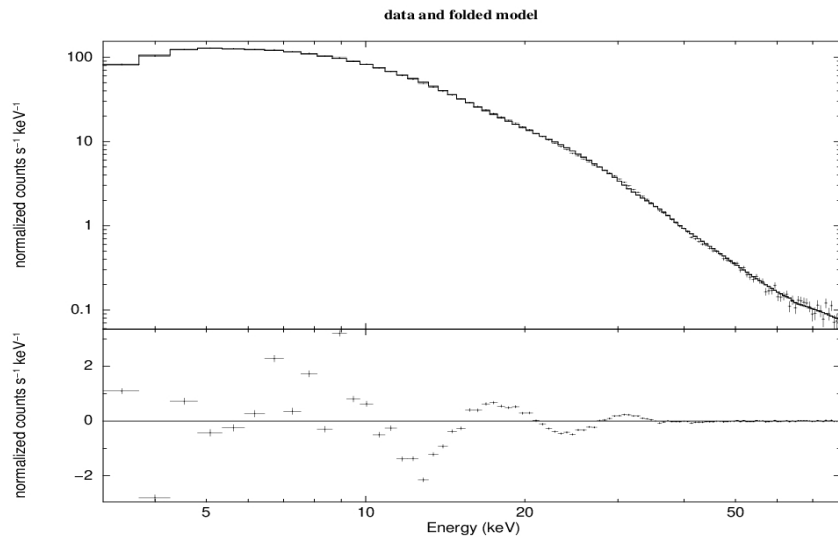
LAXPC 30 : Power Density Spectra of 4U 0115+63 (3-40 keV)



Observed QPO, RMS and Q-factor flux

LAXPC	QPO (Hz) in 3-40 keV, Timescales (sec)	RMS (%)	Q-FACTOR	FLUX (3-80 keV) ergs/cm ² /s
10	9.63E-04, (6.78E-04 1.32E-03) 1038, (1474, 756)	29.4	5.3	1.3214e-08 (2.298e-09–7.427e-09)
	1.73E-03, (1.29E-03 2.035E-03) 575, (774, 492)	19.7	2.4	
20	9.60E-04, (6.37E-04 1.36E-03) 1042, (1568, 732)	18.9	5.2	1.0931e-08 (3.586e-10–2.307e-09)
	1.72E-03, (1.27E-03 2.03E-03) 580, (783, 492)	19.7	2.4	
30	9.65E-04, (5.72E-04–1.43E-03) 1035, (1749, 695)	18.2	7.1	1.1227e-08 (1.212e-11 – 1.172e-08)
	1.71E-03 (1.17E-03 2.16E-03) 582, (849, 463)	19.4	1.97	

Spectral Study of LAXPC 20 (3-80 keV)



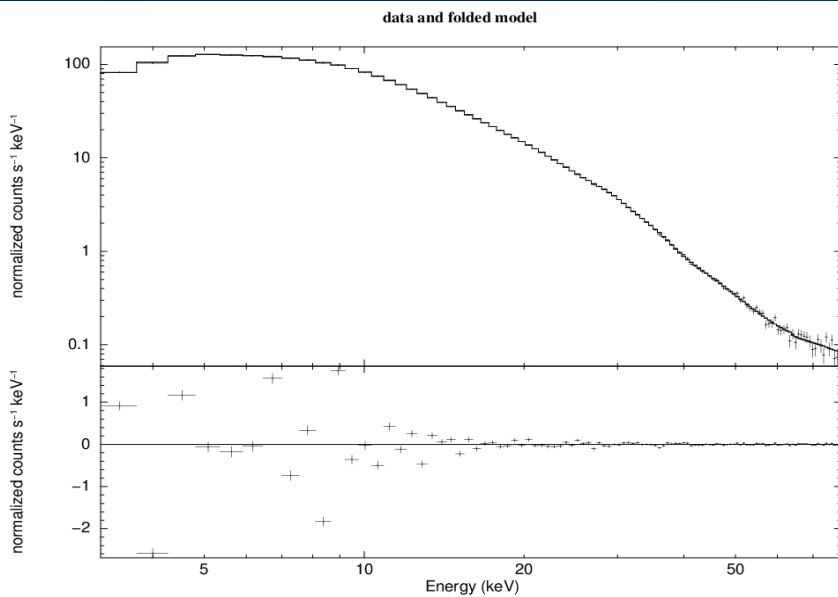
model TBabs(gaussian + cutoffpl + powerlaw)

Cutoffpl Photon Index : 0.22 (+/- 1.87E-02)

Highcut : 10.1 (+/- 0.13)

Powerlaw Photon Index : -2.5 (+/- 0.65)

Reduced chi sq: 5.58 (585.80 for 105 dof)



model Tbabs (gaussian + powerlaw)

cyclabs*cyclabs*cyclabs*cyclabs*cyclabs

Powerlaw Photon Index : 0.91 (-0.32, 0.07)

Reduced chi sq: 0.93 (85.6 for 92 dof)

Flux 1.1008e-08 ergs/cm²/s (1.009e-08 – 1.085e-08), Luminosity at 7kpc; 6.4538e+37 ergs/s

CYCLOTRON LINE & HARMONICS energies

12.9 (-0.39, 0.33)

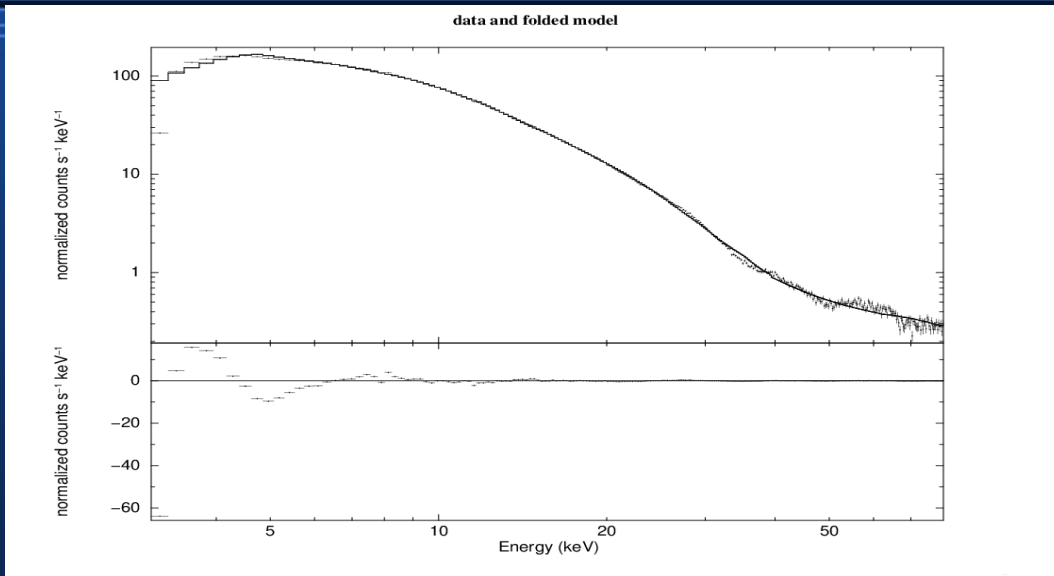
25.1 (-1.28, 1.21)

37.6 (-1.16, 0.88)

41.5 (-1.32, 1.22)

53.1 (-5.7, 7.0)

Spectral Study of LAXPC 30 (3.5-80 keV)



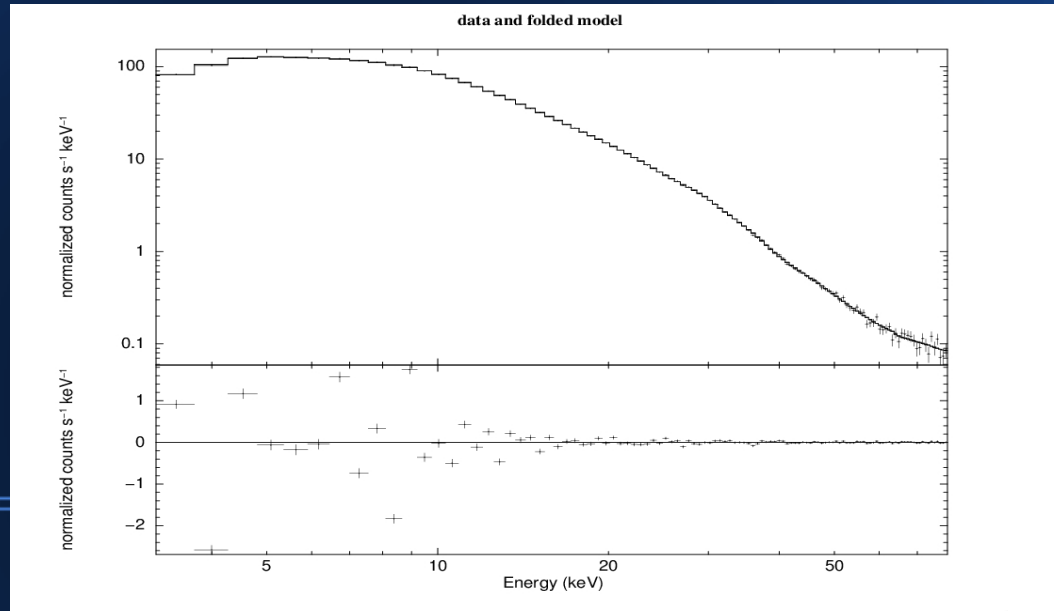
model TBabs(gaussian + cutoffpl + powerlaw)

Cutoffpl Photon Index : 0.75 (+/- 2.92E-02)

Highecut : 9.21 (+/- 0.14)

Powerlaw Photon Index : -1.04 (+/- 7.74E-02)

Reduced chi sq: 23.9 (6680.14 for 287 dof)



model Tbabs*edge (gaussian + powerlaw)

cyclabs*cyclabs*cyclabs*cyclabs*cyclabs

Powerlaw Photon Index : 0.93 (-0.61, 0.46)

Reduced chi sq: 1.12 (279.8 for 263 dof)

Flux $1.0697e-08$ ergs/cm²/s (6.759e-09 – 1.831e-08) Luminosity at 7kpc; $6.2715e+37$ ergs/s

CYCLOTRON LINE & HARMONICS energies

11.2 (-0.40, 0.73)

22.0 (-0.47, 0.84)

35.0 (-0.29, 0.35)

48.6 (-0.33, 0.36)

67.9 (-0.57, 1.12)